ELSEVIER

Cement and Concrete Composites **20** (1998) 1–11

Printed in Great Britain
0958-9465/98/$19.00

PII:S0958-9465(97)00061-9

Flexural Behaviour of Concrete Beams Reinforced with GFRP Bars

Saleh Hamed Alsayed

Department of Civil Engineering, King Saud University, Riyadh 11421, Saudi Arabia

(Received 3 November 1996; accepted 7 October 1997)

Abstract

This study presents the results of the comparison made between the predicted and the measured load–deflection relationships for 12 concrete beams reinforced either by steel or glass fibre reinforced plastic (GFRP) bars. The numerical part of the study was carried out using: (i) the computer model which accounts for the actual properties of the composite constituents developed as part of this study, (ii) the ACI load–deflection model, and (iii) the modified load–deflection model available in the literature for beams reinforced by FRP bars. The last two models were implemented on a spreadsheet. The deflection limit and the ultimate strength of concrete were the control parameters in design of the test beams. The computer model provides an accurate prediction of the measured service and full load–deflection curves. The errors in prediction of service load deflection and ultimate flexural strength are less than 10% and 1%, respectively. In the case of GFRP reinforced beams, the service load deflection predicted by the ACI model is in error by 70%, while that predicted by the modified model is in error by less than 15%. © 1998 Elsevier Science Ltd. All rights reserved.

Keywords: FRP reinforcement, beams, GFRP bars, structural behaviour, service load deflection, ultimate load, analytical model.

NOMENCLATURE

A_s	Area of tension reinforcement (mm^2)
b	Width of cross-section (mm)
c	Distance from extreme compression fibre to neutral axis (mm)
E_p	Modulus of elasticity of FRP reinforcement (MPa)
E_s	Modulus of elasticity of steel reinforcement (MPa)
f_c'	Compressive strength of concrete (MPa)
f_y	Yield strength of steel reinforcement (MPa)
h	Overall thickness of member (mm)
L	Span length of the beam
M_{cr}	Cracking moment (N mm)
M_n	Nominal moment (N mm)
MSLD	Measured service load deflection (mm)
MUL	Measured ultimate load (kN)
MV	Measured values
NA	Neutral axis of the cross-section
PLSD	Predicted service load deflection (mm)
PUL	Predicted ultimate load (kN)
PV	Predicted values
SL	Service load (kN)
ε_c	Top fibre concrete strain
ε_{cu}	Top fibre concrete strain corresponding to ultimate load
ε_{cmax}	Maximum specified value for the top fibre concrete strain
κ	Curvature of the beam (rad)
Δ	Vertical deflection at the beam centreline (mm)
ϕ	Strength reduction factor
ρ	Actual reinforcement ratio
ρ_p	Ratio of GFRP tension reinforcement
ρ_s	Ratio of steel tension reinforcement

INTRODUCTION

There are many existing methods available for preventing, delaying, or repairing the deterioration of concrete structures due to the corrosion of reinforcing steel. However, these methods are costly and their long time effectiveness is not assured.[1] A better and a more innovative solution to the corrosion problem is to eliminate one of the contributing ingredients, i.e. steel, oxygen, or water. This can be achieved by replacing steel with fibre reinforced plastics (FRP).

Lately, the interest in the use of composite materials for civil engineering applications has increased. However, guidance to their use needs to be developed. In recent years, therefore, a number of researchers have studied the behaviour of beams with FRP rods as reinforcement in bending.

Nawy *et al.*[2] examined the behaviour of glass fibre reinforced concrete beams. They included a study of cracking, deflection, reinforcement stress, and ultimate load of 20 tested beams reinforced with different reinforcement ratios of GFRP bars. Failure of most of the glass fibre reinforced test beams occurred in the compression zone due to the compression failure of the concrete rather than the tensile failure of the GFRP bars.

Nakano *et al.*[3] conducted a research using continuous Aramid fibre bars, continuous carbon fibre bars and deformed steel bars. They found that the bending stiffness, after initial cracking, in general, increases with increase in the reinforcement ratio and the modulus of elasticity of the bars.

Nawy & Neuwerth[4] carried out a study on the behaviour of glass fibre reinforced concrete slabs and beams. They reported that once the concrete cracked, the beams deflected at a faster rate for a unit increase in load. Also they observed that by increasing the percentage of tensile reinforcement from 0.7% to 1.4%, the load at the allowable deflection of $L/180$ of the span increased by about 25%.

Faza & GangaRao[5,6] studied the load–deflection behaviour of FRP reinforced concrete (FRP-RC) beams by extending the current methods used for steel reinforced beams to compute post-cracking deflections in FRP-RC beams. Based on the test results, the authors proposed a modified effective moment of inertia, I_m, expressed as a function of the effective moment of inertia, I_e, and the moment of inertia of the cracked transformed section, I_{cr}. Thus, I_m replaces I_e in the calculation of deflection by ACI-318[7] procedure for conventionally reinforced beams. The theoretical and experimental results were very close, showing that the modified equation for computing the moment of inertia of FRP reinforced concrete beams is accurate to predict the deflection of FRP reinforced beams.

Since the stress–strain curve of FRP bars does not have a yield plateau, the possibility of having a failure due to rupture of the FRP bars, which is more brittle than the failure due to crushing of concrete,[8] should be avoided. Therefore, researchers recommend some reduction factors to be applied to the FRP ultimate tensile strength, f_{pu}. Faza & GangaRao[9] recommend that the maximum permissible strength, f_{py}, be 0.80 of the ultimate strength. Nanni[10] suggested that the strength reduction factor, ϕ, be taken as 0.70 and the minimum FRP ratio, ρ_{pmin}, be the larger of $1.33\rho_{pbal}$ (where ρ_{pbal} is the balanced FRP ratio) and $0.24\sqrt{f_c'}/f_{pu}$ (to assure that $\phi M_n > M_{cr}$), where f_{pu} is the tensile strength of the GFRP bars and M_n and M_{cr} are the nominal and cracking moment of the cross-section, respectively. Other researchers[11–13] recommended the use of some allowance (reduction factor) ranging from 0.70 to 0.80.

These studies clearly show that the behaviour of concrete beams reinforced with FRP is different from that of beams reinforced with steel. This necessitates the need for developing altogether new design code provisions or revising the current ones to account for the properties of FRP materials. However, before incorporating the FRP bars into the design codes and standards, extensive research is needed to determine the values and the limitations of these design parameters.

This paper presents the results of the comparisons made between the numerical and experimental load–deflection relationship of nine concrete beams reinforced by GFRP bars and three by steel bars. The numerical computations were carried out using three models. Namely, the computer model that was developed as part of this study, the spreadsheet that was developed considering the currently practised ACI model for the load–deflection relationship up to the service load,[7] and the spreadsheet that was developed considering the model suggested by Faza & GangaRao[5] to pre-

dict the same load–deflection relationship of FRP-RC beams. The variables considered in the experimental study include the reinforcing material type (steel vs GFRP), the deflection limit at service load, and the concrete ultimate compressive strength.

DESIGN OF FRP-RC BEAMS

Flexural strength

The flexural strength of a singly-reinforced beam section according to the ACI-Code provisions[7] requires $M_u \leq \phi M_n$, in which M_u is the required ultimate moment, M_n is the nominal moment capacity of the beam section, and ϕ is the strength reduction factor ($\phi = 0.90$ for flexure). For the FRP-RC section, as explained earlier, a compressive failure is preferred and M_n can be written as:

$$M_n = 0.85 f_c' ab\left(d - \frac{a}{2}\right) \tag{1}$$

where f_c' is the compressive strength of concrete, b is the beam width, d is the effective depth of the cross-section, and a is the stress-block depth. In case of compression failure, it can be shown that:

$$c = \left[\sqrt{m\rho_p + \left(\frac{m\rho_p}{2}\right)^2} - \frac{m\rho_p}{2}\right] d \tag{2}$$

where c is the depth of the neutral axis, m is a material parameter, $(E_p \varepsilon_{cu})/(0.85\beta_1 f_c')$, E_p is the modulus of elasticity of the FRP material, ε_{cu} is the strain at the extreme compression fibre of the concrete, β_1 is the ratio of the stress-block depth to the neutral axis depth, and ρ_p is the FRP ratio.

Ductility requirements

The ductility requirements of the ACI-Code provisions limit the steel ratio $\rho_s = A_s/bd$ to lower and upper limits of $\rho_{smin} = 1.4/f_y$ (where f_y is in MPa) and $\rho_{smax} = 0.75\rho_{sbal}$, respectively, in which ρ_{sbal} is the balanced steel reinforcement ratio given as:

$$\rho_{sbal} = \frac{0.85\beta_1 f_c'}{f_y} \frac{0.003E_s}{0.003E_s + f_y} \tag{3}$$

The balanced reinforcement ratio expression for FRP, ρ_{pbal}, becomes:

$$\rho_{pbal} = \frac{0.85\beta_1 f_c'}{0.67 f_{pu}} \frac{0.003E_p}{0.003E_p + 0.67 f_{pu}} \tag{4}$$

where f_{pu} is the ultimate tensile strength of FRP bar ($0.67f_{pu}$ is the usable stress of FRP bar such that the factor of safety against its rupture is 1.5).[14] In addition, to avoid the possibility of having failure due to breaking of FRP bars and to assure that $\phi M_n > M_{cr}$, the minimum FRP reinforcement ratio is assumed to be the larger of ρ_{pbal} and $0.25\sqrt{f_c'}/f_{pu}$. Furthermore, since the failure of FRP bars is of brittle type, there is no upper limit for reinforcement ratio.[14]

Serviceability requirements

The deflection requirements of the ACI-Code [Table 9.5(b)] limit the computed deflection, Δ, to a specified maximum permissible value, Δ_a, which depends on the span length of the beam and the type of the member. Therefore, for simply-supported beam of span L and loaded by two equal concentrated loads ($P/2$ each) symmetrically placed about the beam centreline, the maximum deflection Δ computed at the beam centreline can be written as:

$$\Delta = \frac{Px}{48E_c I_e}(3L^2 - 4x^2) \tag{5}$$

where x is the distance between the support and the point where the load is applied, P is the applied load, and E_c is the modulus of elasticity of the concrete. According to ACI-Code provisions, the effective moment of inertia, I_e, can be determined as follows:

$$I_e = I_g\left(\frac{M_{cr}}{M_a}\right)^3 + I_{cr}\left[1 - \left(\frac{M_{cr}}{M_a}\right)^3\right] \leq I_g \tag{6}$$

where M_{cr} is the cracking moment, M_a is the maximum service moment, I_{cr} is the moment of inertia of the cracked transformed section, I_g is the gross uncracked moment of inertia of the section about the centroidal axis, neglecting the

reinforcement. However, the ACI load–deflection model was developed under the assumption that reinforcement is provided by steel and as such may not provide a reasonable estimate to predict the load–deflection relationship of beams reinforced by FRP. Faza & GangaRao[5] suggested some modifications to the ACI model to account for the properties of the FRP materials. They proposed different modifications for beams subjected to two concentrated point loads, a single point load, and uniformly distributed load. For a simply-supported beam loaded by two concentrated point loads applied at the third points of the beam, the proposed formulae are:

$$I_m = I_g \text{ for } M_a \leq M_{cr} \quad (7)$$

$$I_m = \frac{23 I_{cr} I_e}{[8 I_{cr} + 15 I_e]} \text{ for } M_a \geq M_{cr}$$

EXPERIMENTAL PROGRAMME

Test beams

The tests were carried out on four series of simply-supported beams, namely series A, B, C, and D. Each series consisted of three identical specimens. All the test specimens had a span of 2700 mm, provided with 8 mm diameter steel stirrups at 120 mm spacing, and loaded by two concentrated loads spaced 100 mm on either side of the beam. Table 1 and Fig. 1 show complete details of the specimen cross-sections, type, quantity, and arrangement of the reinforcement for the four series.

On the day of testing, the concrete strength, f_c', for beams in series A, B, and C was 31 MPa and for beams in series D was 41 MPa. The tension steel had a yield stress of 553 MPa, the 12.7 mm (No. 4) GFRP bars had an ultimate stress of 886 MPa, and the 19 mm (No. 6) GFRP had an ultimate stress of 700 MPa. All GFRP bars used in this study were manufactured using the pultrusion process and had spiral winding on the surface.

Beams in series A (henceforth referred to as the control specimens) were reinforced by steel bars and designed in accordance with the requirements of ACI-318[7] for flexure, shear and deflection. They were designed as under-reinforced sections, as shown in Table 1. However, according to eqn 5eqn 6 and ACI-Code [Table 9.5(b)], the service load deflection of series A beams is about 6.5 mm whereas the maximum permissible service load deflection for the 2700 mm span of the simply-supported beam is 9 mm. Beams in series B were reinforced with GFRP bars and designed using the ultimate strength design method for over-reinforced section such that their cross-section and flexural capacity are the same as those of the control specimens (specimens in series A). No limits were imposed on the deflections of the beams in series B. However, since the modulus of elasticity of GFRP bars, E_p, is smaller than that of steel bars, E_s, ($E_p/E_s < 0.25$), deflections of beams in series B are expected to be much more than the corresponding deflections of the control specimens. Also, the area of GFRP bars needed for group B beams, to fulfil the requirement for minimum FRP reinforcement as discussed earlier, is 2.5 times the steel reinforcement needed for the beams in group A (see Table 1). Beams in series C were also reinforced with GFRP bars and were designed with the help of a computer program such that their deflection at service load is limited to the maximum permissible service load deflection of series A beams (9 mm) and the GFRP bars are minimum (see Table 1). Finally, beams in series D were reinforced with GFRP bars and

Table 1. Details of the test beams

Specimen designation	*Cross-section ($h \times b$) (mm)*	*f_c' (MPa)*	*Tension reinforcement*		
			Material type (bars)	*Quantity*	*$(\rho/\rho_{bal})^a$*
A	210 × 200	31	Steel	3 diam. 14 mm	0.68
B	210 × 200	31	GFRP	4 diam. 19 mm	1.34
C	260 × 200	31	GFRP	4 diam. 12.7 mm	0.64
D	250 × 200	41	GFRP	4 diam. 19 mm	0.90

[a] ρ_{bal} = balanced reinforcement ratio computed using eqn 3 for steel bars and eqn 4 for GFRP bars.

designed also with the help of a computer program such that their service load deflection is the same as that of the control specimens and the reinforcing bars are the same as those of series B beams. As the modulus of elasticity of GFRP bars is low, the only practical solution that may fulfil the specified deflection limits for series C and D beams was to increase the depth of the cross-section over that used for series A and B beams.

Preparation of test specimens

All the beams were cast outside the laboratory, covered with burlap, and demoulded approximately 24 h after casting. They were then stored inside the laboratory, subjected to 14 days of intermittent water curing (twice a day) and left to air dry until the day of testing (28 days after casting). Measurements of the applied load, strain in the steel and GFRP bars, and vertical deflection at the midspan of the beams were respectively carried out using load cells, electrical strain gauges, and linear variable differential transformer (LVDT).

NUMERICAL MODELS

The computer model

The main objective of the computer model was to accurately predict the responses of the constituents of the composites whether they are reinforced with steel or FRP. It was developed based on equilibrium and compatibility conditions. To enhance the predicting capability of the model, the variation of stresses and strains over the depth of the cross-section and along the length of the beam was considered. The model also uses a rational stress–strain relationship to represent the actual behaviour of concrete as adopted by Almusallam & Alsayed.[15]

To run the model, all dimensions of the beam and material properties are first input into the computer and then an initial top fibre concrete strain, ε_c, and the location of the neutral axis are assigned. Through some iterations, the values of M_n and the curvature, κ, corresponding to the assumed ε_c and satisfying the compatibility and equilibrium conditions are

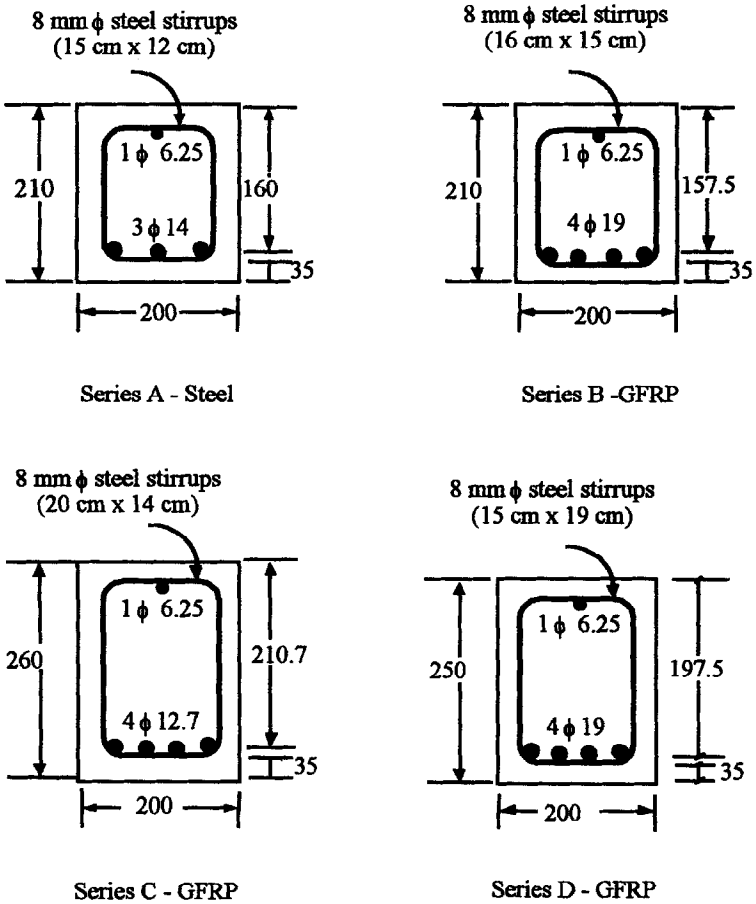

Fig. 1. Cross-section and reinforcement details for beams in series A, B, C, and D.

determined and stored in a vector form. By incrementing ε_c a new set of M_n and κ is then computed. The process of incrementing ε_c, satisfying the compatibility and equilibrium conditions, and generating a set of M_n and κ continued until the maximum specified value for the top fibre concrete strain, ε_{cmax}, is reached (in this study a maximum value of 0.003 was assumed for ε_{cmax}). The stored values of M_n and κ are then used to compute the distribution of the M_n–κ along the length of the beam and the load–deflection relationship is generated. A flow chart for the proposed model is shown in Fig. 2.

The ACI and Faza *et al.* empirical models

In addition to the previously presented computer model, a spreadsheet program which uses the ACI and the Faza & GangaRao[5] numerical procedures was developed to predict the load–deflection relationship of FRP- or steel-RC beams.

TEST RESULTS AND DISCUSSION

Load–deflection behaviour

The average load–deflection curves (each curve represents the average of three curves) for the beams in series A, B, C, and D are shown in Figs 3–6. These results show that, unlike steel-RC beams, there is a sharp drop in the load–deflection relationship of the GFRP-RC beams just after passing the cracking load. It may be attributed to the effect of the low modulus of elasticity, E_p, of the GFRP bars. When concrete at the tension side of the GFRP-RC beam cracks, the major portion of the tensile force is to be transmitted by the reinforcing bars. However, as the GFRP bars have low E_p, the tensile force that can be developed by them corresponding to the cracking strain is less than that developed by the cross-section before cracking. Thus, upon cracking, a kink is formed in the load–deflection relationship. This phenomenon is also recognised by the analytical model (see Figs 4–6). Thereafter, as the applied strains increase, larger tensile forces are developed in the reinforcing bars and continue until failure occurs. The results shown in Figs 4–6 also show that there are some occasional kinks along the load–deflection curves of the GFRP-RC beams even after cracking. These kinks may, however, be attributed to breakage of some of the fibres of the reinforcing bars as a result of the shear lag effect of the GFRP bars which was evident from the breaking sound heard during testing.

Deflection at service load

The enlarged load–deflection curves for the beams in series A, B, C, and D up to the service load of the control series (assumed to be 20 kN which is about 0.35 of the ultimate load of series A beams) are also shown as part of Figs 3–6. To simplify the comparison, the measured service load deflections corresponding to the 20 kN load are also presented in Table 2. As can be seen in the table, when the applied load is 20 kN, the deflection of the beams in series B is almost twice that of series A beams. It can also be easily observed in Figs 3 and 4 that when the applied load on series B beams is 12 kN (60% of the 20 kN), the deflection at the centrelines of series B beams is the same as the deflection at the centrelines of series A beams when the applied load is 20 kN. This clearly suggests that in situations where the service load deflection is critical, replacing the steel bars with GFRP bars without changing the cross-sectional dimensions may not be a practical alternative.

Furthermore, when the applied load is 20 kN, the deflections at the centrelines of series C and D beams are 8.79 mm and 5.8 mm, respectively. These values are almost, as were designed for, equal to the maximum permissible service load deflection for the simply-supported beam with 2700 mm span and the service load deflection of series A beams, respectively.

Ultimate flexural strength

The average ultimate strengths recorded for the test beams in all series are listed in Table 2. It can be seen in the table that, as were designed for, series A and B attained almost the same ultimate flexural strength, i.e. the ultimate strength design method for over-reinforced section correctly predicted the ultimate strength of the GFRP-RC beams. This substantiates the validity of using the ultimate design method for over-reinforced sections to predict the ultimate strength of a GFRP-RC beam. However, since no deflection limits were imposed on series B

beams, the flexural strength controlled the design. The centreline deflection of series A beams corresponding to the ultimate load is 20 mm, whereas that of the series B beams is

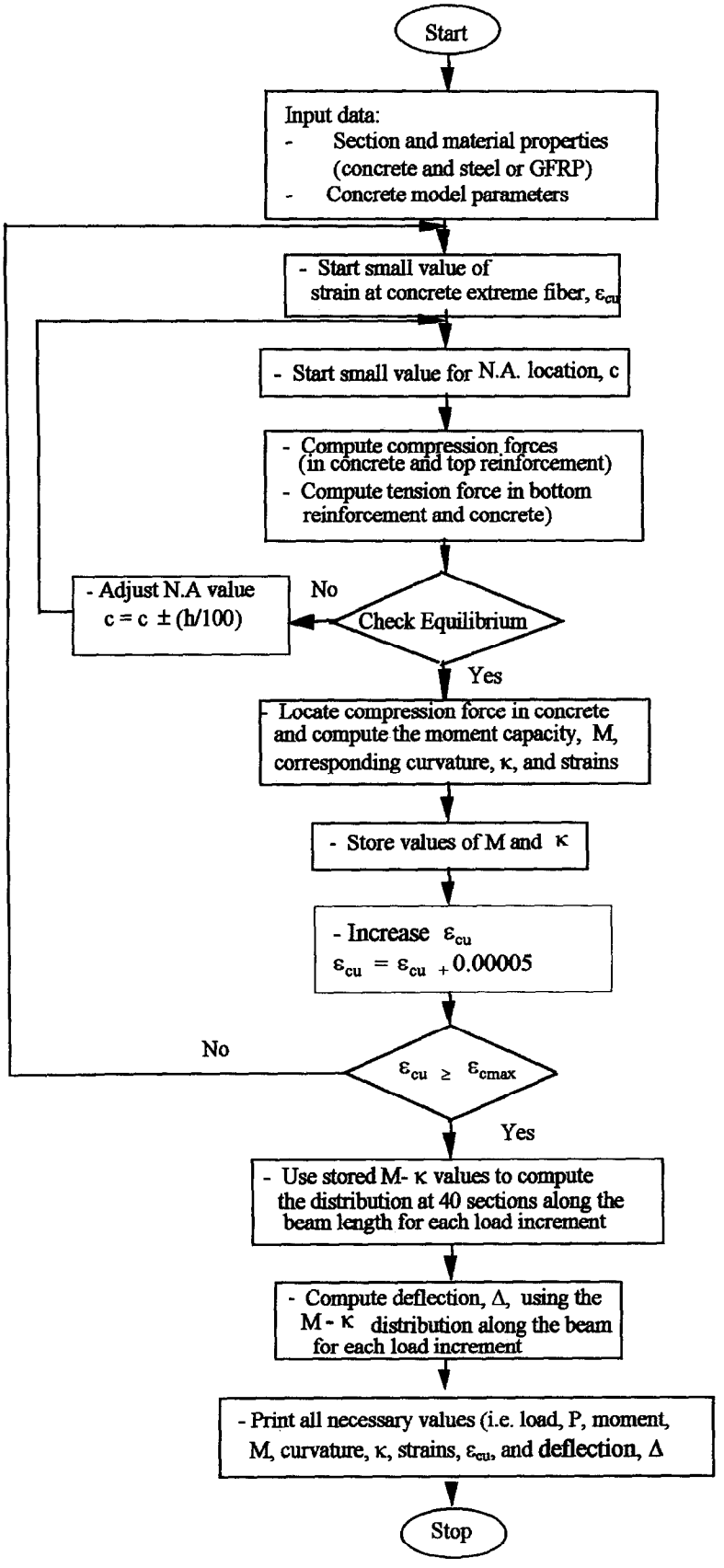

Fig. 2. The flow chart of the analytical.

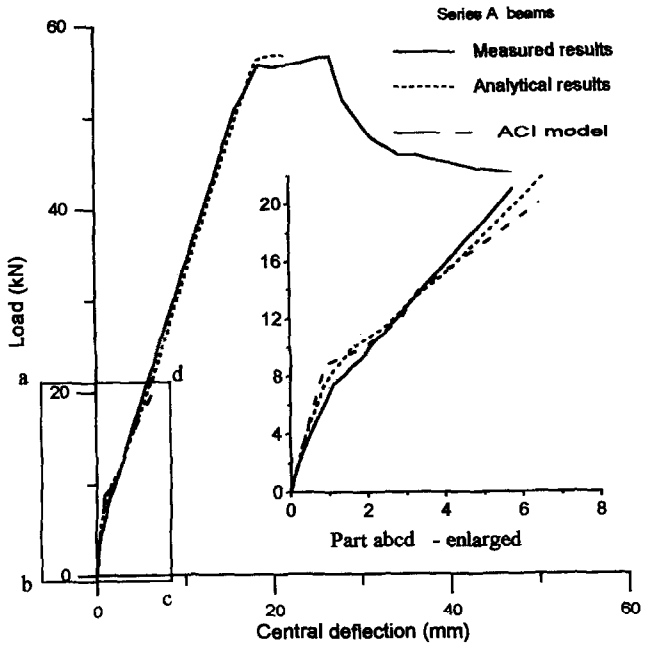

Fig. 3. Load–deflection relationship for series A beams.

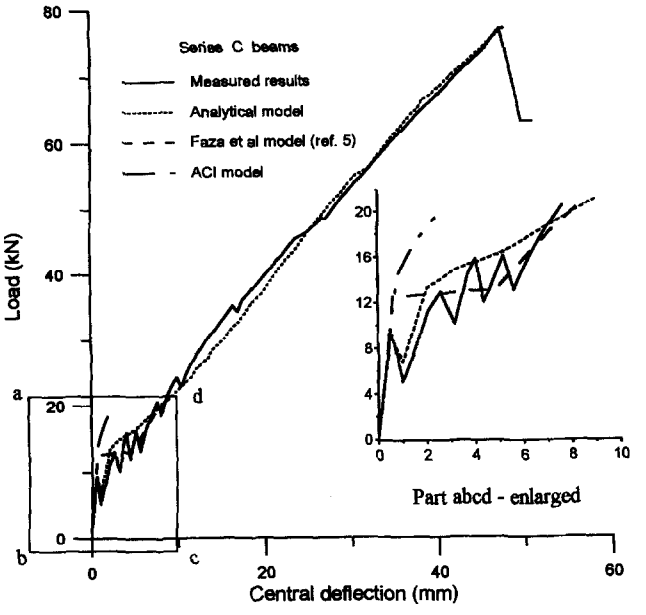

Fig. 5. Load–deflection relationship for series C beams.

39 mm (see Fig. 3Fig. 4). Thus, for the same flexural strength, replacing steel bars with GFRP bars without changing the dimensions of the cross-section resulted in doubling the deflection corresponding to the ultimate load.

On the other hand, as the deflection controlled the design of series C and D beams, they had larger cross-sections than series A beams. Therefore, series C and D beams attained higher loads and deflections at ultimate than those attained by series A beams (see Table 2). The increase in the ultimate loads in series C and D over that of series A are 36 and 53%, respectively. The corresponding increase in the deflections at ultimate are 21 and 36%, respectively.

It is of importance to point out here that since series A beams were under-reinforced sections (see Table 1) their failure started due to yielding of the tension reinforcement followed by concrete crushing. On the other hand, since the beams in series B, C, and D were over-reinforced sections their failure was due to concrete crushing. However, the failure was not sudden, as would have been the case had the failure occurred due to rupturing of the GFRP bars,[8] with deflections reaching values more than 40 mm.

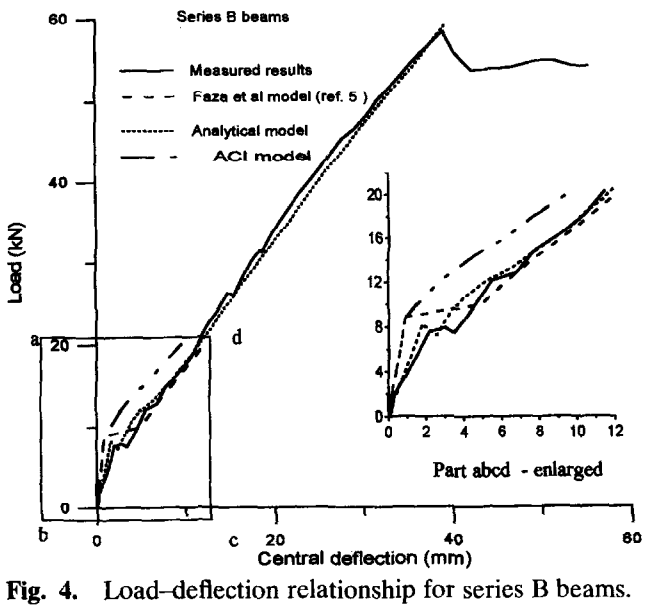

Fig. 4. Load–deflection relationship for series B beams.

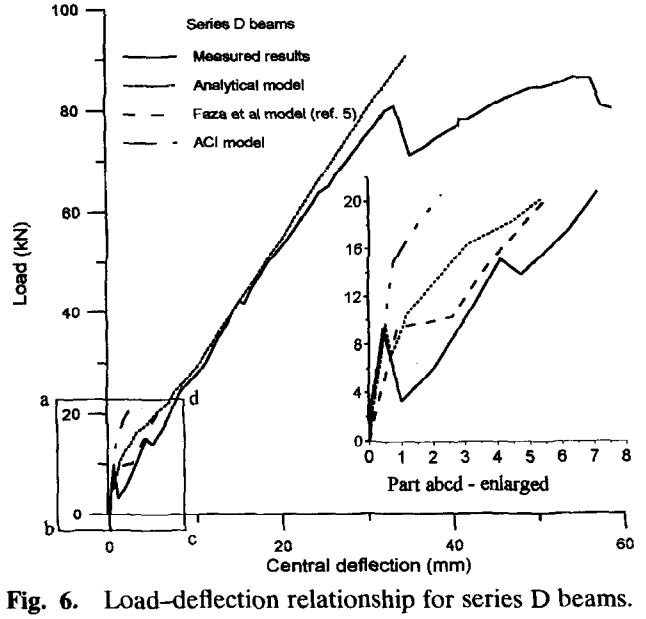

Fig. 6. Load–deflection relationship for series D beams.

Table 2. Measured vs predicted service load deflection and ultimate load

Sequence		*Beam series*			
		A	*B*	*C*	*D*
1	SL (kN)	20	20	20	20
2	MSLD (mm)	5.44	10.64	8.79	5.80
3	PSLD (analytical) (mm)	5.86	11.47	8.14	5.28
4	Ratio of rows 3/2	1.08	1.08	0.93	0.91
5	PSLD (ACI) (mm)	6.44	9.48	2.55	2.08
6	Ratio of rows 5/2	1.18	0.89	0.31	0.39
7	PSLD (Faza) (mm)	—	12.12	7.94	5.46
8	Ratio of rows 7/2	—	1.14	0.90	0.81
9	MUL (kN)	56.54	58.40	76.96	86.37
10	PUL (analytical) (kN)	56.66	59.10	77.00	90.62
11	Ratio of rows 10/9	1.00	1.01	1.01	1.02

COMPARISON BETWEEN MEASURED AND PREDICTED RESULTS

Deflection at cracking load

The predicted and average measured loads and deflections for beams in all series corresponding to their cracking loads are presented in Table 3. The ratios of the predicted to the measured values are also presented in the same table.

Although the quantities at this level of loading are small, the results indicate that for series A beams (reinforced with steel bars), both the ACI and the analytical models reasonably predicted the cracking loads and their corresponding deflections. For the beams in other series (reinforced with GFRP bars) the average errors in predicting the cracking load and deflection using the analytical model are, respectively, 5 and 15% which, for such small quantities, are tolerable. The corresponding errors using the ACI model, and at this level of loading also the Faza *et al.* model, are 33 and 58%. The increase in errors using the ACI model over those encountered using the analytical model may be attributed to the fact that the ACI model does not account for the properties of the GFRP bars which differ from those of the steel bars. Further experimental data are, however, needed before any suggestion can be made in this regard.

Deflection at service load

The predicted and average measured deflections at service loads for beams in all series are presented in Table 2. The results show that the predicted values using the analytical model are in good agreement with the corresponding measured values. The error in predicting the service load deflection in any of the series considered herein is less than 10%. The results also show that the current ACI model underestimates the actual deflection of all GFRP-RC beams. The measured deflection of series C is 245% over that computed by the ACI model, i.e. the service load deflection for beams in series C as computed by the ACI model is only 30% of the corresponding measured deflection. This clearly shows that the current ACI model cannot be

Table 3. Measured vs predicted load and deflection at cracking load

Sequence		*Beam series*							
		A		*B*		*C*		*D*	
		Load	*Deflection*	*Load*	*Deflection*	*Load*	*Deflection*	*Load*	*Deflection*
1	MV (mm)	7.42	1.12	7.56	2.00	9.22	0.56	9.20	0.44
2	PV (analytical)	7.49	0.89	8.19	1.64	9.30	0.49	9.61	0.50
3	PV (ACI)[a]	8.81	0.89	8.81	0.891	3.51	0.72	2.29	0.74
4	Ratio of rows 2/1	1.01	0.80	1.08	0.82	1.01	0.88	1.05	1.14
5	Ratio of rows 3/1	1.19	0.80	1.17	0.45	1.47	1.29	1.35	1.68

[a]The ACI and Faza *et al.*[5] cracking load and deflection were computed considering I_g.

used in its current form to reasonably predict the service load deflection of FRP-RC beams. Results shown in the table also reveal that the predicted service load deflections for the GFRP-RC beams using the Faza *et al.* model[5] are in good agreement with the measured values. The error in predicting the service load deflection of GFRP-RC beams is less than 15%. However, their proposed modification for beams subjected to other types of loading was not validated and, therefore, further experimental results are needed to validate all proposed models considering the influence of different loading configurations, different reinforcement arrangements, and the variation in the properties of the different types of FRP materials. Also, with the help of a computer, some parametric studies should be carried out to refine the proposed empirical models.

Load–deflection curves up to the ultimate load

Load–deflection curves up to ultimate state generated by the proposed analytical model and the corresponding measured curves for beams in all series considered in this study are shown in Figs 3–6. The average ratio of the predicted ultimate flexural strengths (loads) to the corresponding measured values for the beams in all series is about 1 (see row 11 of Table 2). These results clearly show that there is an excellent agreement between the predicted and measured values. This is true for all beams and at all levels of loading which may be regarded as evidence of the capability of the proposed model to predict the actual behaviour of steel as well as GFRP-RC beams. The small deviation between the measured and predicted values that are occasionally seen along the curves may be ascribed to the slippage and shear lag effects which are not accounted for in the analytical model.

CONCLUSIONS

Based on the measured and predicted results obtained in this study, the following conclusions may be drawn.

(1) The current ACI model for predicting the load–deflection relationship for steel-RC beams underestimates the actual deflection of GFRP-RC beams. The error in predicting the actual service load deflection of the GFRP-RC beam is about 70%. Therefore, until more data become available it should not be used for FRP-RC beams.

(2) Replacing the current effective moment of inertia by the modified effective moment of inertia to account for the properties of FRP as proposed by Faza & GangaRao greatly improved the capability of the empirical model to predict the service load deflection of the FRP-RC beams. Such modification reduces the error in predicting the service load deflection from 70% to less than 15%. However, more experimental results are needed to further check the proposed modifications under different load cases, reinforcement configurations, and variations in the properties of the FRP materials.

(3) The proposed computer model is capable of predicting the cracking and service load deflections of steel and GFRP-RC beams. The errors between predicted and measured cracking and service load deflections of the GFRP-RC beams is less than 20 and 10%, respectively.

(4) The developed computer model, as it accounts for the actual properties of the materials that constitute the composite, accurately predicts the load–deflection relationship of steel as well as GFRP-RC beams at all levels of loading. The model can be extended to consider properties of other types of FRP materials and then used to modify the currently practised design formulae that were generated assuming that reinforcement is provided by steel.

(5) For GFRP-RC beams designed to fail by crushing of concrete (compressive failure), the beam capacity in flexure can be reasonably estimated using the ultimate design method for over-reinforced sections. However, the deflection at service load for such beams may control the design of many types of FRP-RC structures. The average ratio of the measured service load deflection of GFRP-RC beams to that of steel-RC beams of the same ultimate flexural capacity and the same dimensions is about 2.

(6) Using a factor of safety of 1.5 against the possibility of tensile failure of GFRP bars

assures a relatively gradual type failure of FRP-RC beams due to concrete compression failure rather than a catastrophic failure due to rupturing of the FRP bars.

(7) As other types of FRP materials have similar shape of stress–strain relationship, the above stated conclusions, with some variations in the numerical values, may hold good for beams reinforced by other types of FRP.

REFERENCES

1. Clarke, J. L., Non-ferrous reinforcement for concrete 2000. In *Proc. Int. Conference 1993, Economic and Durable Construction Through Excellence*, Eds. R. K. Dhir & M. R. Jones, The University of Dundee, Scotland, pp. 229–238.
2. Nawy, E. G., Neuwerth, G. E. & Phillips, C. J., Behaviour of fibre glass reinforced concrete beams. *Journal of the Structural Engineering Division, ASCE*, **97** ST9 (1971) 2203–2215.
3. Nakano, K., Matsuzaki, Y., Fukuyama, H. & Teshigawara, M., Flexural performance of concrete beams reinforced with continuous fibre bars. In *ACI Int. Symposium 1993, Fibre Reinforcement for Concrete Structures*, Ed. A. Nanni, Detroit, MI, pp. 743–751.
4. Nawy, E. G. & Neuwerth, G. E., Fibreglass reinforced concrete slabs and beams. *Journal of the Structural Engineering Division, ASCE*, **103** ST2 (1977) 421–440.
5. Faza, S. S. & GangaRao, H. V. S., Pre- and post-cracking deflection behaviour of concrete beams reinforced with fibre-reinforced plastic rebars. In *Advanced Composite Materials in Bridges and Structures 1992*, Eds. Neale & Labossiere. Canadian Society for Civil Engineering, Montreal, Quebec, pp. 151–160.
6. Faza, S. S. & GangaRao, H. V. S., Bending response of beams reinforced with FRP rebars for varying concrete strengths. In *Proc. ASCE Speciality Conference, 1991, Advanced Composite Materials in Civil Engineering Structures*, Eds. Iyer & Sen. American Society of Civil Engineers, New York, pp. 262–270.
7. ACI Committee 318, Building code requirements for reinforced concrete and commentary (ACI 318-95/ACI 318R-95). American Concrete Institute, Detroit, MI, 1995.
8. Kakizawa, T., Ohno, S. & Yonezawa, T., Flexural behaviour and energy absorption of carbon FRP reinforced concrete beams. In *ACI Int. Symposium 1993, Fibre Reinforcement for Concrete Structures*, Ed. A. Nanni, Detroit, MI, pp. 585–598.
9. Faza, S. S. & GangaRao, H. V. S., Theoretical and experimental correlation of behaviour of concrete beams reinforced with fibre reinforced plastic rebars. In *ACI Int. Symposium 1993, Fibre Reinforcement for Concrete Structures*, Ed. A. Nanni, Detroit, MI, pp. 599–614.
10. Nanni, A., Flexural behaviour and design of RC members using FRP reinforcement. *Journal of the Structural Engineering Division, ASCE*, **119** ST11 (1993) 3344–3359.
11. Saadatmanesh, H. & Ehsani, M. R., Fibre composite bar for reinforced concrete construction. *Journal of Composite Materials*, **25** 2 (1991) 188–203.
12. Faza, S. S. & GangaRao, H. V. S., Bending and bond behaviour of concrete beams reinforced with plastic rebars. *Transportation Research Record, No. 1290*, Vol. 2, Third Bridge Engineering Conference. Transportation Research Board, Washington, DC, 1991.
13. Dolan, C. W., Kevlar reinforced prestressing for bridge decks. *Transportation Research Record, No. 1290*, Vol. 1, Third Bridge Engineering Conference. Transportation Research Board, Washington, DC, 1991.
14. Alsayed, S. H. & Al-Salloum, Y. A., Optimization of flexure environment of concrete beams reinforced with fiber reinforced plastic rebars. *Magazine of Concrete Research*, **48** 174 (1996) 27–36.
15. Almusallam, T. H. & Alsayed, S. H., Stress–strain relationship of normal, high strength and light weight concrete. *Magazine of Concrete Research*, **47** 170 (1995) 39–44.